

# Construction of autotrophic nitrogen removal system based on zero-valent iron (ZVI): performance and mechanism

Han Yang, Liangwei Deng, Youqian Xiao, Hongnan Yang, Hong Wang and Dan Zheng

## ABSTRACT

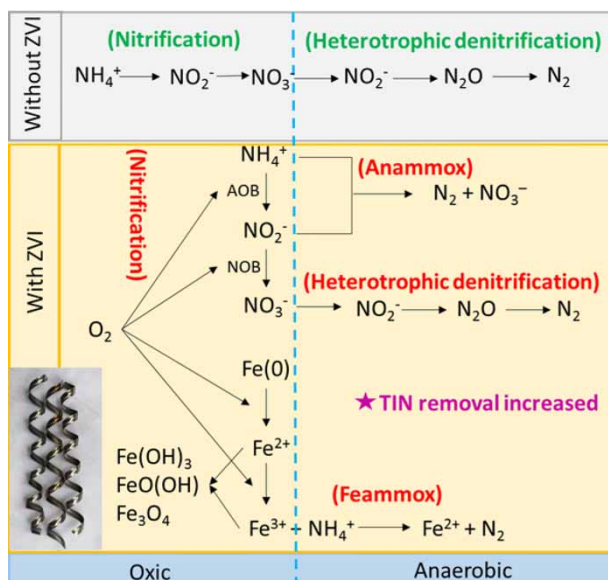
In this study, the performance and mechanism of nitrogen removal in sequencing batch reactors (SBRs) with and without zero-valent iron (ZVI) was investigated. The results showed that ZVI had a capacity to promote  $\text{NH}_4^+$ -N conversion,  $\text{NO}_2^-$ -N accumulation and total inorganic nitrogen (TIN) removal, with the TIN removal rate being increased by 29.45%. The ZVI also had a significant impact on microbial community structure by means of high-throughput pyrosequencing, increasing the enrichment of Anammox (anaerobic ammonium oxidation) bacteria *Candidatus Brocadia* and Feammox (anaerobic ferric ammonium oxidation) bacteria *Ignavibacterium*. With ZVI addition, the main pathway of nitrogen removal was changed from nitrification-heterotrophic denitrification to Anammox and Feammox.

**Key words** | Anammox, autotrophic denitrification, Feammox, zero-valent iron

## HIGHLIGHTS

- ZVI can promote  $\text{NH}_4^+$ -N conversion,  $\text{NO}_2^-$ -N accumulation and TIN removal.
- ZVI can increase the enrichment of Anammox and Feammox bacteria.
- ZVI was beneficial to the construction of autotrophic denitrification system.

## GRAPHICAL ABSTRACT



doi: 10.2166/wst.2020.544

**Han Yang**  
**Liangwei Deng**  
**Youqian Xiao**  
**Hongnan Yang**  
**Hong Wang**  
**Dan Zheng** (corresponding author)  
 Biogas Institute of Ministry of Agriculture and Rural Affairs,  
 Chengdu 610041,  
 China  
 and  
 Laboratory of Development and Application of Rural Renewable Energy,  
 Ministry of Agriculture and Rural Affairs,  
 Chengdu, 610041,  
 China  
 E-mail: zhengdan@caas.cn

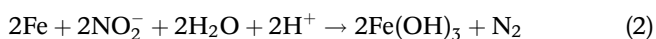
**Han Yang**  
 Chengdu Drainage Limited Liability Company,  
 Chengdu 610000,  
 China

## INTRODUCTION

A large amount of wastewater containing a high concentration of  $\text{NH}_4^+\text{-N}$  is produced during fermentation processes used to treat wastes and wastewaters from livestock and poultry breeding enterprises, and also from pharmaceutical, chemical and other industries. Discharge of the wastewater without further treatment to remove nitrogen would cause serious pollution problems, such as eutrophication and acid rain (Windey *et al.* 2005; Wang *et al.* 2012). At present, biological treatment is the main method for nitrogen removal (Scott *et al.* 2013; Qian *et al.* 2014). The traditional biological nitrogen removal method is nitrification combined with heterotrophic denitrification, in which nitrifying bacteria oxidize  $\text{NH}_4^+\text{-N}$  to  $\text{NO}_2^-\text{-N}$  and  $\text{NO}_3^-\text{-N}$  under aerobic conditions, and then heterotrophic denitrifying bacteria reduce  $\text{NO}_3^-\text{-N}$  and  $\text{NO}_2^-\text{-N}$  into  $\text{N}_2$  using organic carbon sources under hypoxic conditions (Schinner *et al.* 1996; Obaja *et al.* 2003). However, some wastewaters with high concentrations of  $\text{NH}_4^+\text{-N}$  are also characterized by a low C/N ratio and the lack of organic carbon source as an electron donor during denitrification, thus resulting in poor denitrification performance (Foglar & Briški 2003; Kartal *et al.* 2010).

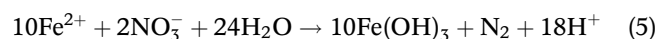
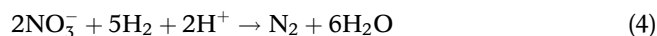
In recent years, the autotrophic denitrification process (based on using inorganic sources as electron donation) has provided an alternative nitrogen removal approach in the field of wastewater treatment. The known electron donors include ammonia (Kartal *et al.* 2010), sulfide (Batchelor & Lawrence 1978), hydrogen (Lee & Rittmann 2003), zero-valent iron (ZVI) (Till *et al.* 1998), ferrous iron, etc.

The nitrogen removal process involving iron (Fe) has long been studied. ZVI can be directly used as an electron donor for denitrification and the processes are shown as Equations (1) and (2):

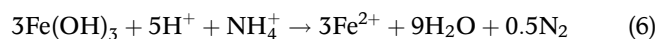


Under anaerobic conditions,  $\text{H}_2$  and  $\text{Fe}^{2+}$  being generated from the corrosion of ZVI by autotrophic microorganisms can be used as electron donors for the reduction of  $\text{NO}_3^-\text{-N}$  and  $\text{NO}_2^-\text{-N}$  to  $\text{N}_2$  (Till *et al.* 1998; Wang *et al.* 2012). The theoretical stoichiometric expressions

describing this process are shown as Equations (3)–(5):



$\text{Fe}^{2+}$  is readily oxidized to  $\text{Fe}^{3+}$  in the presence of oxidizing agents or iron-oxidizing bacteria. Anaerobic ferric ammonium oxidation (Feammox), in which  $\text{NH}_4^+\text{-N}$  is directly oxidized to  $\text{N}_2$  when  $\text{NH}_4^+\text{-N}$  is used as the electron donor and  $\text{Fe}^{3+}$  is the acceptor, has also attracted increasing attention. This reaction is described by Equation (6) (Yang *et al.* 2012):



The processes described by Equations (1)–(6) provide new opportunities for the development and application of novel biological nitrogen removal technologies related to iron. Fe in various valence states has been used in research on wastewater treatment using sequencing batch reactors (SBRs), and good treatment performances have been reported. For example, Anammox start-up time has been shortened from 126 days to 105 days and 84 days with the addition of mZVI and nZVI, respectively; furthermore, the nitrogen removal was improved remarkably (Ren *et al.* 2015). Wang *et al.* (2018) used ZVI to remedy acidification and deterioration during aerobic post-treatment of digested effluent; they found total inorganic nitrogen (TIN) removal efficiency dramatically improved (from 1.83% to 93.3%) (Wang *et al.* 2018). Although some studies have achieved good nitrogen removal efficiency, the nitrogen removal mechanism of reaction system after adding ZVI remains unclear.

SBRs integrate aerobic and anaerobic processes, thus the reaction mechanisms in the SBR system are complicated. Nitrification may occur under aerobic conditions, and anaerobic-related reactions may occur in anaerobic conditions, such as Anammox, heterotrophic denitrification, and Feammox. Therefore, it is meaningful to explore the pathway and mechanism of nitrogen removal in the SBR reactor after adding ZVI.

The objective of this study was to reveal the mechanism of autotrophic denitrification in SBRs mediated by ZVI

through the study of Fe/N conversion stoichiometry and the analysis of microbial community structure. The study objective was focused on determining: (1) whether ZVI can be used to screen autotrophic microorganisms and to promote the rapid construction of autotrophic nitrogen removal system or not; (2) how the addition of ZVI affects the autotrophic N removal system; and (3) what are the main nitrogen removal pathways in the new ZVI autotrophic denitrification system and what are the functional microorganisms that play important roles.

## MATERIALS AND METHODS

### Seed sludge, synthetic wastewater, and ZVI

Seed sludge was taken from an aerobic tank of a municipal wastewater treatment plant in Chengdu, Sichuan Province, People's Republic of China., and the mixed liquor volatile suspended solids (MLVSS) concentration was 5.43 g/L and was used to inoculate wastewater at a ratio of 1:1 (v:v). The reactors were fed with synthetic wastewater. The synthetic wastewater was prepared with tap water and primarily contained 100–400 mg/L  $\text{NH}_4^+\text{-N}$ , 2 g/L  $\text{KHCO}_3$ , 0.01 g/L  $\text{KH}_2\text{PO}_4$ , 0.00423 g/L  $\text{CaCl}_2$  and 0.3 g/L  $\text{MgSO}_4$ . In addition, 1 mL per liter of the following trace elements solutions were added to synthetic wastewater: 6.25 g/L

$\text{FeSO}_4\cdot 7\text{H}_2\text{O}$  and 5 g/L EDTA (in solution I); and 0.99 g/L  $\text{MnCl}_2\cdot 4\text{H}_2\text{O}$ , 15 g/L EDTA, 0.43 g/L  $\text{ZnSO}_4\cdot 7\text{H}_2\text{O}$ , 0.014 g/L  $\text{H}_3\text{BO}_3$ , 0.25 g/L  $\text{CuSO}_4\cdot 5\text{H}_2\text{O}$ , 0.19 g/L  $\text{NiCl}_2\cdot 6\text{H}_2\text{O}$ , 0.24 g/L  $\text{CoCl}_2\cdot 6\text{H}_2\text{O}$ , and 0.22 g/L  $\text{NaMoO}_4\cdot 2\text{H}_2\text{O}$  (in solution II).

ZVI used in the experiment consisted of iron scraps collected from a mechanical processing factory. Each piece of scrap was 10–20 cm long, 1–5 mm wide and 1–2 mm thick. The scrap had a Fe content of 96.52% and C content of 3.48%, as determined in a previous study (Wang *et al.* 2018).

### Experimental set up

The experimental set up was shown in Figure 1. Two circular SBR reactors made of glass were used with a working volume of 2 L each (50 cm high, 8 cm in diameter). One aerator was installed at the bottom of each reactor to maintain the dissolved oxygen (DO) concentration at  $1.0 \pm 0.3$  mg/L during aeration. The temperature of reactors were both maintained at 30 °C using a constant temperature water bath. Peristaltic pumps were used for feeding influent and discharging effluent. Reactors had a hydraulic retention time (HRT) of 4 days. The reactors used intermittent aeration with 1 h of aeration followed by 2 h of precipitation, and a cycle of 24 hours (including 15 min of feeding, 8 h of aeration, 15.5 h of settling and 15 min of drainage). The feeding volume of each cycle was 0.5 L. ZVI (30 g/L) was

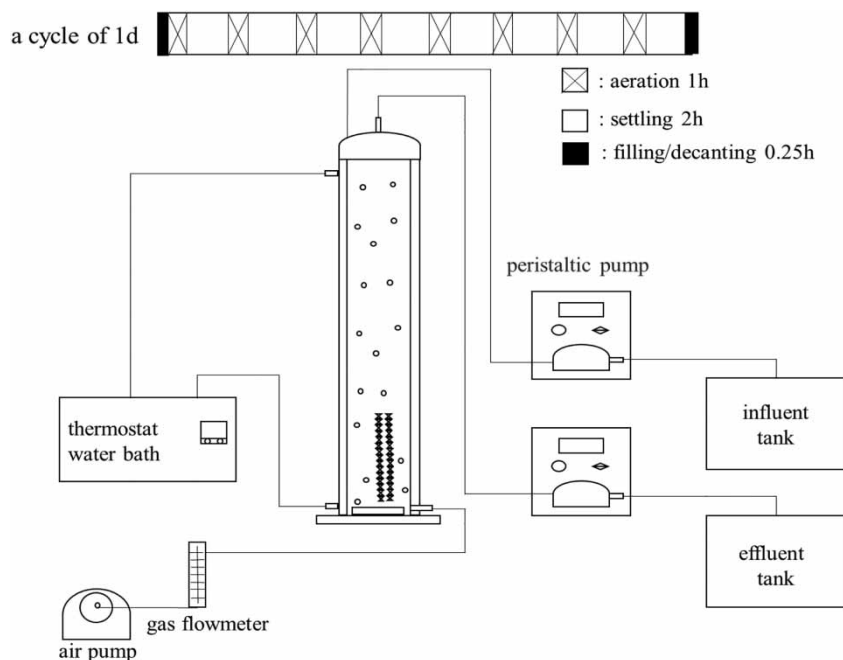


Figure 1 | Experimental set up of SBR based on ZVI.

added into one reactor (named R30), and the other reactor (named R0) was operated as a control without added ZVI.

### Analytical methods

Samples from the two SBRs were taken periodically (every other day) for routine analysis according to standard methods (APHA 2012). Concentrations of  $\text{NH}_4^+\text{-N}$ ,  $\text{NO}_2^-\text{-N}$ , and  $\text{NO}_3^-\text{-N}$  were analyzed using an auto-analyzer (AA3; Bran + Luebbe, Norderstedt, Germany). DO and pH were measured using an online continuous-monitoring auto analyzer (MIQ/TC2020XT; WTW Company, Germany). Concentrations of  $\text{Fe}^{2+}$  and total iron ion concentrations ( $\text{Fe}^{x+}$ ) were measured by O-phenanthroline spectrophotometry.  $\text{Fe}^{3+}$  concentration was calculated as the difference between the concentrations of  $\text{Fe}^{x+}$  and  $\text{Fe}^{2+}$ .

The iron scrap was removed from the reactor at the end of operation, and drained with a vacuum freeze dryer (SCIENTZ-12ND, China). The samples were then observed using a scanning electron microscope (SEM, Hitachi SU1510, Japan). The composition and proportion of elements were determined by energy dispersive X-ray spectroscopy (EDS, HORIBAEX-250, Japan) and SEM.

### High-throughput pyrosequencing

Triplicate sludge samples were taken from the two reactors (R0/R30) at the end of operation (day 110). In addition, the inoculated sludge (named RS) was also analyzed. All genomic DNA of samples was extracted using an E.Z.N.A. Soil DNA Kit (Omega) following the manufacturer instructions under required aseptic conditions. The quality, integrity, and concentration of each DNA sample was determined by 1% agarose gel electrophoresis and a NanoDrop ND-2000 spectrophotometer (Thermo Fisher Scientific). Libraries were prepared following the 16S Metagenomic Sequencing Library Preparation protocol from Illumina. Briefly, the region V4 from 16S rRNA was amplified using primers 515F/806R (515F GTGCCAGCMGCCGCGGTAA; 806R GGACTACHVGGGTWTCTAAT) to which Illumina Sequencing adapters and dual-index barcodes of the Nextera XT kit were added. The pair-end library construction and sequencing of 16S rDNA amplicons was carried out using an Illumina HiSeq 2500 sequencing platform using a  $2 \times 250$  bp-end protocol.

Raw sequences were de-multiplexed, trimmed, and filtered to remove low-quality reads using the open-source software system Quantitative Insights into Microbial Ecology (QIIME) quality filters (Caporaso *et al.* 2010).

Chimeric sequences were checked by UCHIME and removed from subsequent analyses. Then, all the merged sequences were mixed to pick OTUs with an identity threshold of 97% using the UPARSE pipeline (Edgar 2013). The representative sequences for each OTU, RDP classifier tools and the Silva database were used to obtain the taxonomic information for the OTUs. The normalized OTU abundance profile was generated for downstream analysis on the assumption that the raw OTU read counts were rarefied to the same counts for each sample. Based on the normalized OTU abundance profile, the four alpha diversity indices (Chao1, Shannon, Observed-species and PD-whole-tree) were calculated to estimate the species diversity and richness for each sample using QIIME software (Caporaso *et al.* 2010). The distances of microbial communities between different samples were calculated using Bray-Curtis. Weighted and unweighted UniFrac beta-diversity metrics dissimilarity on microbial community structure was evaluated by nonparametric multivariate analysis of similarity (ANOSIM) and Multi Response Permutation Procedure (MRPP) (Lozupone & Knight 2005; Yoshioka 2008). Metastat analysis was performed to find OTUs that exhibited significant differences between groups, based on Fisher's exact test and FDR calibration (White *et al.* 2009).

## RESULTS AND DISCUSSION

### Effect of ZVI added on nitrogen conversion

The operation duration of SBRs was 110 days and consisted of four stages (A/B/C/D) divided according to different influent  $\text{NH}_4^+\text{-N}$  concentrations (Table 1). As shown in Figure 2(a), the effluent  $\text{NH}_4^+\text{-N}$  concentration from R30 and R0 was always less than 5 mg/L in stages A and B, and the  $\text{NH}_4^+\text{-N}$  removal efficiency almost always exceeded 98%. It is noteworthy that there was only a small difference in the effluent  $\text{NH}_4^+\text{-N}$  concentrations of the two reactors ( $p > 0.05$ ), and that the  $\text{NH}_4^+\text{-N}$  removal efficiency of R0 was slightly higher than that of R30. These results indicated that ammonium-oxidizing bacteria were sensitive to ZVI, and the bacteria were at the adaptive stage. Previous research has shown similar results. Cullen *et al.* (2011) observed that  $\text{NH}_4^+\text{-N}$  oxidation potential appeared to be inhibited by an nZVI dose of 10 mg/g soil on days 0–3 and was accompanied by  $\text{NO}_2^-\text{-N}$  production, but then recovered (Cullen *et al.* 2011).

At the beginning of stage C, the influent  $\text{NH}_4^+\text{-N}$  increased to 300 mg/L, the  $\text{NH}_4^+\text{-N}$  removal efficiency of

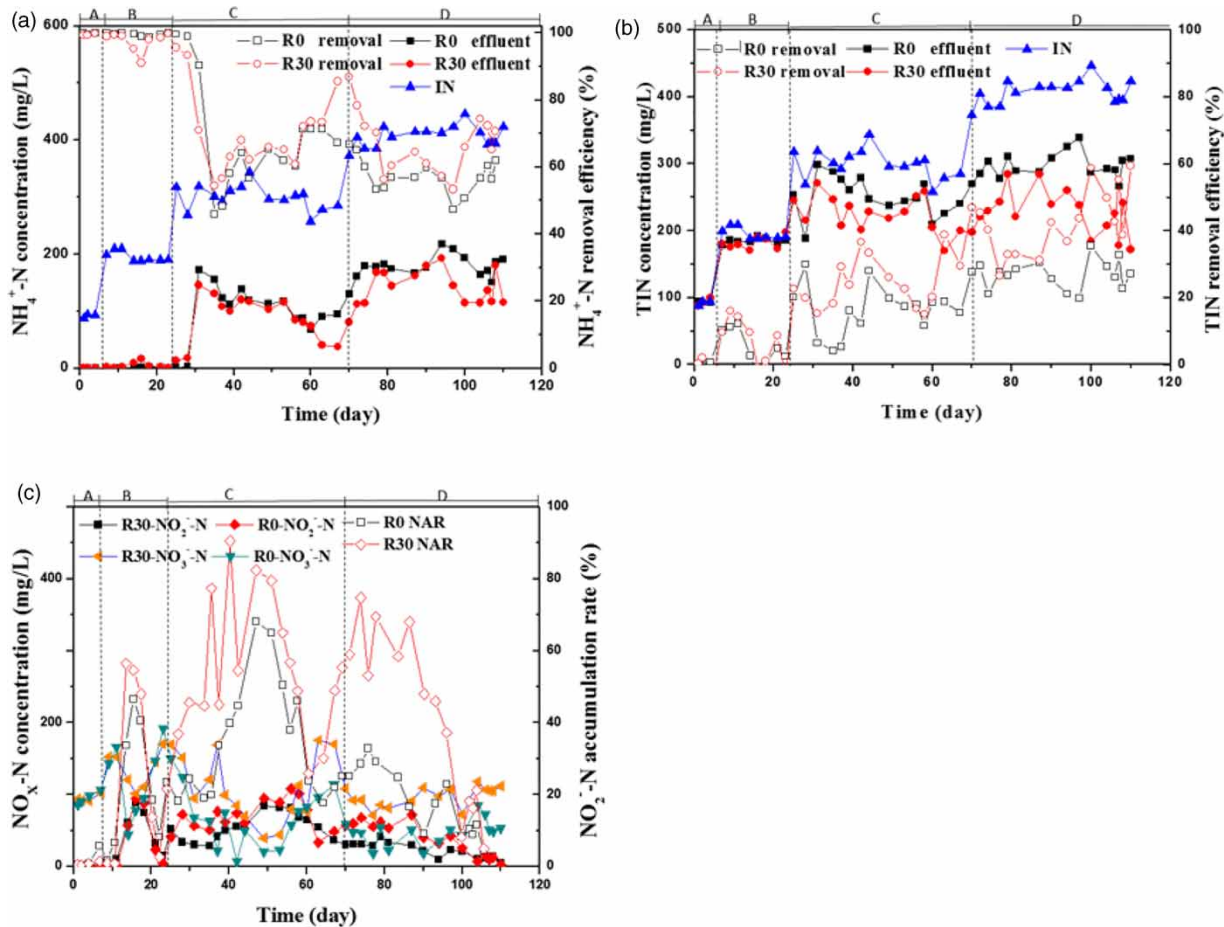
**Table 1** | Operating procedure and parameters for SBRs treating synthetic wastewater

Stages	Time (d)	ZVI addition (g/L)		Influent $\text{NH}_4^+\text{-N}$ (mg/L)	HRT (d)	Influent pH	Aeration DO (mg/L)
		R0	R30				
A	0–7	0	30	$100 \pm 10$	4	$8.5 \pm 0.1$	$1.0 \pm 0.3$
B	8–21	0	30	$200 \pm 10$	4	$8.2 \pm 0.1$	$1.0 \pm 0.3$
C	22–70	0	30	$300 \pm 10$	4	$8.2 \pm 0.2$	$1.0 \pm 0.3$
D	71–110	0	30	$400 \pm 10$	4	$8.0 \pm 0.1$	$1.0 \pm 0.3$

the two reactors decreased. The  $\text{NH}_4^+\text{-N}$  removal efficiency of R30 was higher than that of R0 (reaching a maximum of 88%). In stage D,  $\text{NH}_4^+\text{-N}$  removal in both reactors decreased slightly and the  $\text{NH}_4^+\text{-N}$  removal efficiency of R30 always exceeded that of R0. With the increase of  $\text{NH}_4^+\text{-N}$  load in the inlet water, the  $\text{NH}_4^+\text{-N}$  removal load of two reactors also increased in the whole operation process and R30 with ZVI addition was significantly higher than of R0 without ZVI in stages C and D. These results indicated that ZVI added at a dosage of 30 g/L was better

able to withstand the impact of high  $\text{NH}_4^+\text{-N}$  load and to promote  $\text{NH}_4^+\text{-N}$  oxidation.

Figure 2(b) shows that the TIN removal efficiency in both reactors gradually increased as operation time increased. In stage A, the efficiency of removing TIN in both reactors was less than 10% ( $p > 0.05$ ), and nitrification was the dominant process. In stage B, TIN removal efficiency of R30 generally exceeded that of R0, and this difference was even more obvious during stage C, for which statistical analyses showed significant difference

**Figure 2** | The nitrogen removal performance of SBRs without added ZVI (R0) and with added ZVI (R30): (a) concentration and removal efficiency of  $\text{NH}_4^+\text{-N}$ ; (b) concentration and removal efficiency of TIN; (c) concentration of  $\text{NO}_2^-\text{-N}$  and  $\text{NO}_3^-\text{-N}$  ( $\text{NO}_x\text{-N}$ ) and  $\text{NO}_2^-\text{-N}$  accumulation rate (NAR).

( $p < 0.05$ ). Compared with the TIN removal efficiency of R0 (20.67%), that of R30 (50.12%) was increased by 29.45%. The addition of ZVI significantly improved TIN removal, which was consistent with previous studies. For example, Wang et al. (2018) observed that 60 g/L ZVI addition improved TIN removal efficiency from 1.83% to 93.3% in a process treating digested effluent (Wang et al. 2018).

ZVI went through anaerobic and aerobic stages in the SBR system.  $H_2$  and  $Fe^{2+}$  were produced by corrosion of ZVI, and these could be used as electron donors for  $H_2$ -based autotrophic denitrification and  $Fe^{2+}$ -based autotrophic denitrification, respectively (Till et al. 1998; Biswas & Bose 2005). Compared with the process in R0, the addition of ZVI in R30 increased the amount of electron donors available for denitrification in the system, and significantly improved the removal of TIN.

The effluent  $NO_2^-$ -N concentration of R30 was higher than that of R0, and the  $NO_2^-$ -N accumulation rate was higher than that of R0 (Figure 2(c)), indicating that ZVI exerted a certain inhibitory effect on  $NO_2^-$ -N oxidizing bacteria (NOB), and was conducive to the accumulation of  $NO_2^-$ -N (which was the substrate for Anammox). According to Equation (1), ZVI in water generated  $Fe^{2+}$  could be used as an electron donor for  $NO_2^-$ -N autotrophic reduction, resulting in the  $Fe^{2+}$  being oxidized to  $Fe^{3+}$ .

### Effect of ZVI on acid-base environment of SBR system

The pH of the influent was stable in the range 8.0–8.2. In stage A, the effluent pH was always higher than the influent pH and exhibited a small difference between the two reactors (Figure 3). At the initial stage of autotrophic

denitrification, a large amount of organic matter still existed when the sludge was inoculated. During the degradation of the aerobic organic matter, the aerobic respiration phosphorylation process of micelles continuously absorbed  $H^+$ . Furthermore, the low  $NH_4^+$ -N concentration in the reactors in the first two stages resulted in only a small amount of  $H^+$  being generated. Therefore, the consumption of  $H^+$  was stronger than the release of  $H^+$  through nitrification, thus leading to increasing pH. In stage C, the acid production increased with the increasing influent  $NH_4^+$ -N concentration, and the consumption weakened; thus, pH began to decrease. Although previous studies have reported that iron can react with  $H^+$  to improve the alkalinity of the system (Wang et al. 2018), this was not the case in this study. In stage C, the effluent pH of R30 was lower than that of R0. However, the range of pH fluctuations in R30 (generally between 6 and 7.5) was smaller than that in R0 (which reached as high as 8, and continued to decline in the later stage to as low as 5.5).

$Fe^{2+}$  existed at all stages of operation. The SBR has both aerobic and anaerobic states.  $Fe^{2+}$  generated through ZVI corrosion was the electron donor of nitrate reduction, then  $Fe^{2+}$  was oxidized to  $Fe^{3+}$ . The  $Fe^{2+}$  can also be oxidized to iron oxide in the aerobic phase. The stable existence of  $Fe^{2+}$  could be determined in the system, and with running,  $Fe^{2+}$  gradually reduced, which indicated that an iron oxide passivation layer was formed on the surface of ZVI, which further impeded the corrosion of ZVI iron and produces  $Fe^{3+}$ . Therefore, the content of  $Fe^{3+}$  can be used as an indication of the degree of corrosion of ZVI.

As shown in Figure 4, aqueous  $Fe^{x+}$  were mainly  $Fe^{3+}$ , and their concentration gradually decreased as the duration

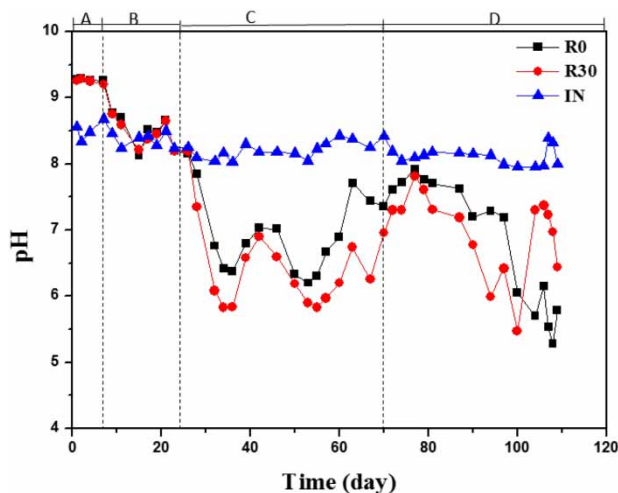


Figure 3 | Variations of pH in SBRs without added ZVI (R0) and with added ZVI (R30).

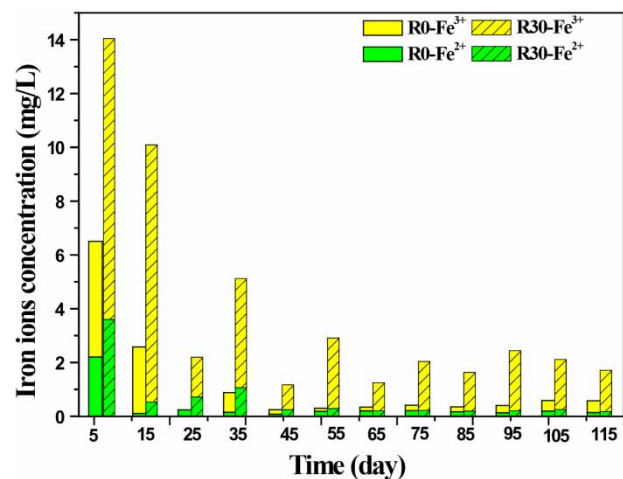


Figure 4 | Variations of  $Fe^{2+}$  and  $Fe^{3+}$  concentrations in SBRs without added ZVI (R0) and with added ZVI (R30).

of SBR operation increased. This occurred mainly because a passivation layer formed on the surface of the ZVI after reaction, which prevented the continuous dissolution of internal  $\text{Fe}^{2+}$ . The morphological changes of ZVI before and after the reaction are illustrated in Figure 5. Before being added to the SBR system, the surface of ZVI was

flat and smooth. After the reaction, corrosion traces were obvious and regular crystalline substances formed. As shown in Figure 6 and Table 3, the energy spectrum analysis of the ZVI confirmed that the elemental iron composition of ZVI decreased from 86.32% before the reaction to 62.94% after the reaction, and the content of elemental oxygen

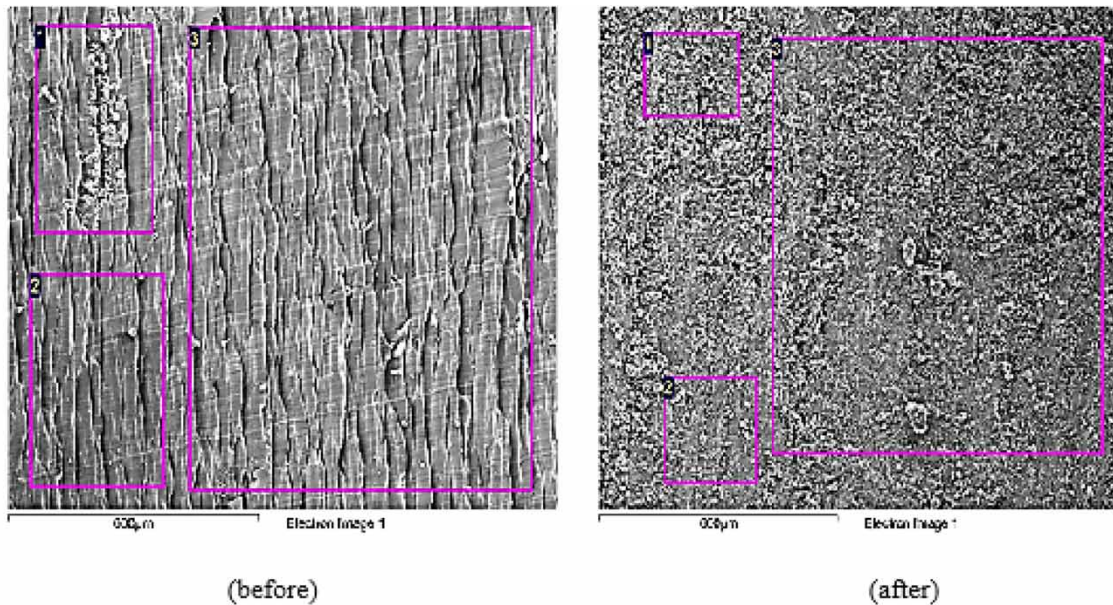


Figure 5 | Scanning electron microscope imagery of iron scraps before and after reaction.

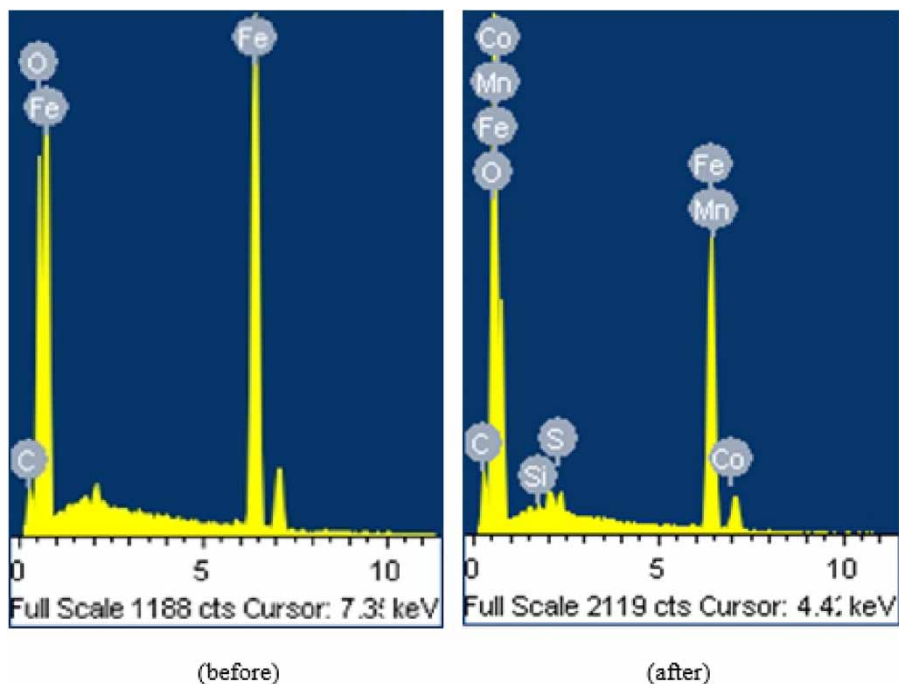


Figure 6 | Elemental composition of iron scraps before and after reaction.

Table 2 | Performance of SBRs without added ZVI (R0) and with ZVI (R30)

Parameters	Stage A (1-7 d)			Stage B (8-21 d)			Stage C (22-70 d)			Stage D (71-110 d)		
	R0	R30	p value	R0	R30	p value	R0	R30	p value	R0	R30	p value
Effluent $\text{NH}_4^+\text{-N}$ (mg/L)	0.43	0.77		0.69	1.46		114.86	95.52		180.10	144.13	
$\text{NH}_4^+\text{-N}$ removal efficiency (NRE, %)	99.69	99.52	> 0.05	99.59	98.06	> 0.05	66.70	73.00	> 0.05	57.00	67.24	< 0.05
$\text{NH}_4^+\text{-N}$ removal load ( $\text{kg}/(\text{m}^3\cdot\text{d})$ )	0.0138	0.0138		0.0277	0.0272		0.0278	0.0304		0.0316	0.0374	
Effluent $\text{NO}_2^-\text{-N}$ (mg/L)	0.53	0.60		13.71	6.67		56.30	71.62		21.73	37.55	
Effluent $\text{NO}_3^-\text{-N}$ (mg/L)	93.08	92.63		177.47	162.67		165.63	139.13		119.77	86.53	
Nitrite accumulation rate (NAR, %)	0.57	0.63		13.60	11.31		34.66	53.33		18.40	42.56	
$\text{TIN}^{\text{a}}$ removal efficiency (%)	1.32	3.32	> 0.05	2.80	2.97	> 0.05	17.65	30.97	< 0.05	27.50	48.49	< 0.05
$\text{TIN}^{\text{a}}$ removal load ( $\text{kg}/(\text{m}^3\cdot\text{d})$ )	0.0002	0.0005		0.0078	0.0082		0.0074	0.0129		0.0153	0.0269	

<sup>a</sup>Total Inorganic Nitrogen; R0: reactor without ZVI; R30: reactor with ZVI.

increased from 10.80% to 28.97%. These results indicated that ZVI mainly generated ferroxidase compounds that were attached to the surface of the ZVI, and a small amount also existed in the form of free aqueous  $\text{Fe}^{x+}$ .  $\text{Fe}_3\text{O}_4$  has been reported as a common product in Fe (0)-oxidation by oxygen or nitrate (Liu et al. 2018).  $\text{FeO}(\text{OH})$  and  $\text{Fe}(\text{OH})_3$  were also the main iron compounds that could be transferred and stored in the extracellular polymeric substance of microorganisms (Arcon et al. 2012).

### Effect of ZVI on microbial community structure

After domestication, the microbial community structure in the reactors changed significantly. The Shannon indexes for RS, R0 and R30 were 7.95, 6.05 and 5.77, respectively (Table 4). The microbial diversity of both R0 and R30 decreased compared with that of RS, and the diversity of the microbial community in R30 was smaller than that of R0. At the genus level (Table 5 and Figure 7), the dominant microorganisms in RS were aerobic bacteria such as *Nitrosomonas* with relative abundance (RA) of 12.5%, anaerobic fermentation bacteria *Limnobacter* (RA of 3.81%), *Clostridium sensu stricto* (RA of 3.67%), *Woodsholea* (RA of 2.25%), *Truepera* (RA of 1.94%), *Comamonas* (RA of 1.91%) and similar microorganisms. After domestication and cultivation in the inorganic environment, the microbial community in the reactors changed from containing mainly heterotrophic bacteria (in RS) to containing mainly autotrophic bacteria, with most heterotrophic microorganisms decreasing in abundance. *Nitrosomonas*, *Nitrospira* and *Nitrospira* were identified as ammonium oxidizing bacteria (AOB) and NOB. As the reaction time increased, the RA of NOB increased from 0.08% (in RS) to 22.72% (R30) and 24.5% (R0), and the relative abundance of AOB in R30 (10.32%) was much higher than that of R0 (3.03%).

In general, the abundance of nitrifying bacteria in R0 and R30 obviously increased compared to RS. This change may indicate that the inorganic environment was more conducive to the growth of NOB. In another study, heterotrophic aerobic bacteria proliferated in the presence of organic matter and had a high RA in the activated sludge system, competing with nitrifying and other aerobic bacteria for oxygen, thereby inhibiting the growth of the nitrifying bacteria (Sohn et al. 2006; Liu et al. 2010). When their environment changed from organic (i.e. RS) to inorganic (the SBRs), most heterotrophic bacteria were gradually eliminated, and nitrifying bacteria gradually increased in abundance, becoming the dominant microorganisms.

**Table 3** | Elemental composition of iron scraps before and after reaction

Sample	In stats	C	O	Si	S	Mn	Fe	Co	Total
Before reaction	Yes	1.96	10.05	–	–	–	87.99	–	100.00
After reaction	Yes	5.05	29.35	0.47	0.64	0.84	63.56	0.08	100.00

**Table 4** | Microbial community statistics of Alpha diversity indexes

Samples	Shannon	Chao1	Observed-species	PD-whole-tree
RS	7.95	3,034.87	2,720	137.50
R0	6.05	2,496.40	2,149	103.51
R30	5.77	2,442.47	2,098	105.66

**Table 5** | Relative abundance of microbial community at genus level in inoculated sludge (RS) and in SBRs without added ZVI (R0) and with added ZVI (R30)

Genus name	RS (%)	R0 (%)	R30 (%)
<i>Nitrospira</i>	0.08	24.47	22.72
<i>Nitrosomonas</i>	12.50	3.03	10.33
<i>Nitrosospira</i>	1.44	1.61	0.05
<i>Candidatus Brocadia</i>	0	1.68	10.45
<i>Ignavibacterium</i>	0.02	0.37	12.77
<i>Thermomonas</i>	0.79	4.06	0.77
<i>Limnobacter</i>	3.81	2.83	1.61
<i>Clostridium sensu stricto1</i>	3.67	1.97	1.15
<i>Comamonas</i>	1.92	0.22	0.18
<i>Truepera</i>	1.95	0.16	0.15
<i>Turcibacter</i>	1.52	1.08	0.67
<i>Filimonas</i>	0.70	0.52	0.24
<i>Woodsholea</i>	2.25	0.06	0.02

Nitrifying bacteria have a complex intramembrane fold structure, and  $\text{Fe}^{x+}$  can increase the permeability of the cell membrane, thus accelerating the absorption of nutrients (Wang *et al.* 2003; Li *et al.* 2004). This study showed that the proper amount of iron can accelerate nitrification in an activated sludge system. Some of the biodegradable organic matter was available to heterotrophic microorganisms in R0 whose RAs were higher than those of R30, such as anaerobic fermentation bacterium *Clostridium sensu stricto* (RA of 1.96%), *Turcibacter* (RA of 1.08%) and *Filimonas* (RA of 0.53%). The nitrogen removal bacteria in R0 were mainly heterotrophic denitrifiers, for instance, *Thermomonas* (RA of 4.05%), *Limnobacter* (RA of 2.83%), *Clostridium sensu stricto* (RA of 1.97%) and *Comamonas* (RA of 0.22%), and were also among the same dominant

species in RS. However, the bacterial community in R0 was significantly different from that of R30, in which the Anammox bacteria *Candidatus Brocadia* (RA of 10.45%) and heterotrophic microorganism *Ignavibacterium* (RA of 12.74%) were significantly enriched, compared to their abundance in R0 (*Candidatus Brocadia* of 1.68% and *Ignavibacterium* of 0.37%). In another study, *Ignavibacterium* was reported as a type of Feammox microorganism that gained energy by reducing  $\text{Fe}^{3+}$  to  $\text{Fe}^{2+}$  (Iino *et al.* 2010).

The addition of ZVI was beneficial to the enrichment of Anammox bacteria, which was due to  $\text{Fe}^{2+}$  production in the process of ZVI corrosion. Other researchers have shown that the addition of 0.09 mM  $\text{Fe}^{2+}$  can significantly increase the quantity of Anammox bacteria. Ferrous ions were highly relevant to hydrazine dehydrogenase activity and increased the quantity of Anammox bacteria (Bi *et al.* 2014). In the present study, the ZVI changed the dominant species from heterotrophic denitrifying bacteria to autotrophic Anammox bacteria and Feammox bacteria. ZVI had a great influence on the microbial community structure and affected the critical pathway and mechanism of nitrogen removal. These results also indicated that despite acclimation in an inorganic environment, the dominant species of denitrifying microorganisms in R0 remained unchanged, but the relative abundance of species did change.

### Mechanism of ZVI addition mediating nitrogen removal in SBR

The above results showed that the addition of ZVI had a promoting effect on nitrogen conversion and total nitrogen removal, and could change the microbial community structure. Therefore, the mechanism of nitrogen removal based on ZVI addition is worthy to be analyzed.

The bacteria in R0 were mainly nitrifying bacteria, including *Nitrospira*, *Nitrosomonas*, *Nitrosospira* and heterotrophic denitrifying bacteria of *Thermomonas*, *Limnobacter* and some heterotrophic microorganisms such as anaerobic fermentation bacteria of *Clostridium sensu stricto* and *Turcibacter*. This bacterial community composition indicated that the nitrogen removal pathway in the

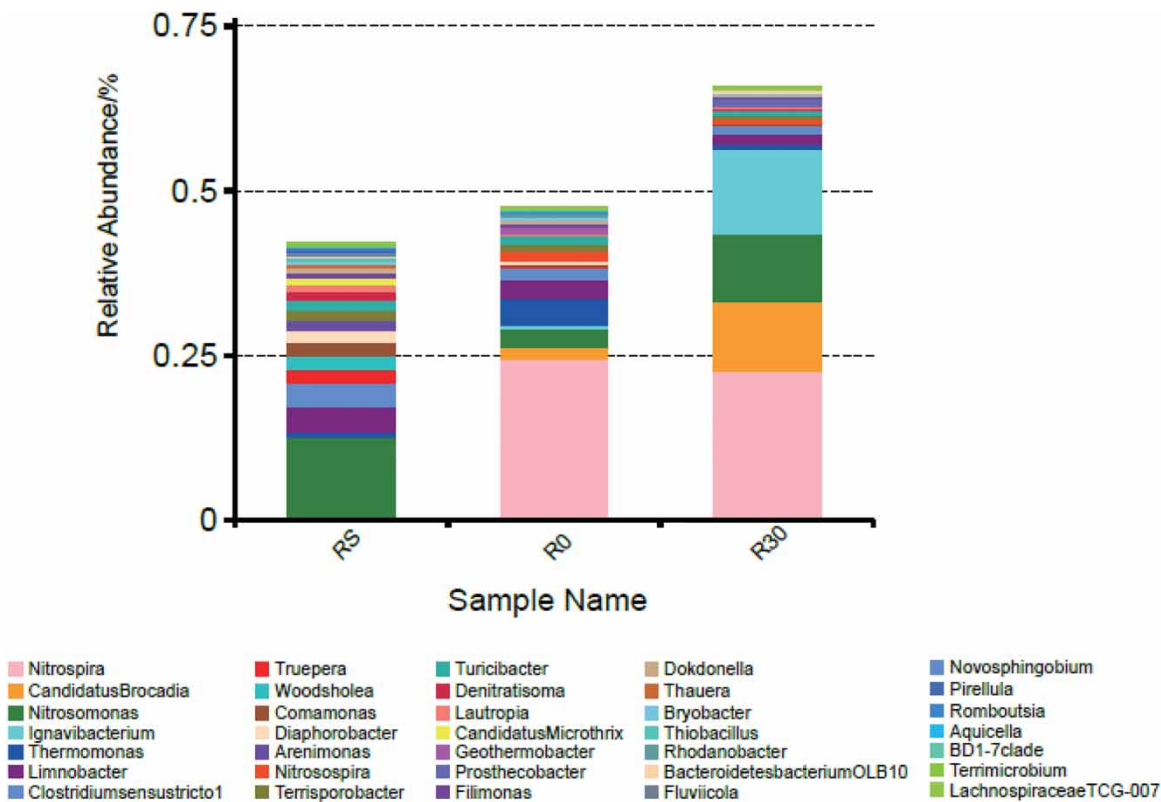


Figure 7 | Relative abundance of most abundant 35 bacterial species at genus level.

absence of ZVI was mainly traditional nitrification-heterotrophic denitrification. Moreover, due to the lack of organic carbon in the wastewater, the main carbon source was the residual organic matter of dead microbial cells during the process of acclimation.

Thus, the total nitrogen removal performance in R0 was poor. In contrast, the significant enrichment of the Anammox bacteria *Candidatus Brocadia* in R30 suggested that the Anammox process was one of the main denitrification pathways in R30 for nitrogen removal. Iron, mainly in the form of iron-sulfur protein, is an indispensable element for microbial metabolism and growth. Nevertheless, its traces for the majority of bacteria and the threshold value is lower than bacteria, which is iron-dependent redox. Anammox bacteria rely heavily on iron-containing proteins (especially cytochromes) for their energy conservation, which occurs within a unique organelle, the anammoxosome (Ferousi et al. 2017). Other researchers have reported that divalent iron can shorten the start-up time of an Anammox reactor and promote the enrichment of Anammox bacteria; for example, 0.09 M of  $\text{Fe}^{2+}$  shortened the start-up time of the Anammox process from 70 d to 50 d (Bi et al. 2014).

ZVI promotes the enrichment of Anammox bacteria, accelerates the construction of the autotrophic denitrification system, and improves nitrogen removal efficiency. In addition, *Ignavibacterium*, a heterotrophic microorganism that gains energy by reducing trivalent ferric iron, was highly abundant in R30 compared to its presence in R0. Wang et al. (2016) reported that *Ignavibacterium* may be a functional microorganism of the Feammox process. Thus, it can be inferred that Feammox also contributed considerably to nitrogen removal in R30 (Wang et al. 2016).

In addition, the abundance of NOB in R30 was less than that in R0, but the RA of AOB in R30 was greater than that of R0. These observations were consistent with the higher accumulation rate of  $\text{NO}_2^-$ -N and greater  $\text{NH}_4^+$ -N conversion in R30 than in R0. ZVI may have had a slight inhibitory effect on NOB, thus promoting the accumulation of  $\text{NO}_2^-$ -N and the Anammox process. Analysis of microbial species and different nitrogen removal processes in this study, including total nitrogen removal,  $\text{NH}_4^+$ -N conversion,  $\text{NO}_2^-$ -N accumulation, etc., further confirmed that the main nitrogen removal process in R0 was nitrification-heterotrophic denitrification, while Anammox and Feammox were important processes in ZVI-amended R30.

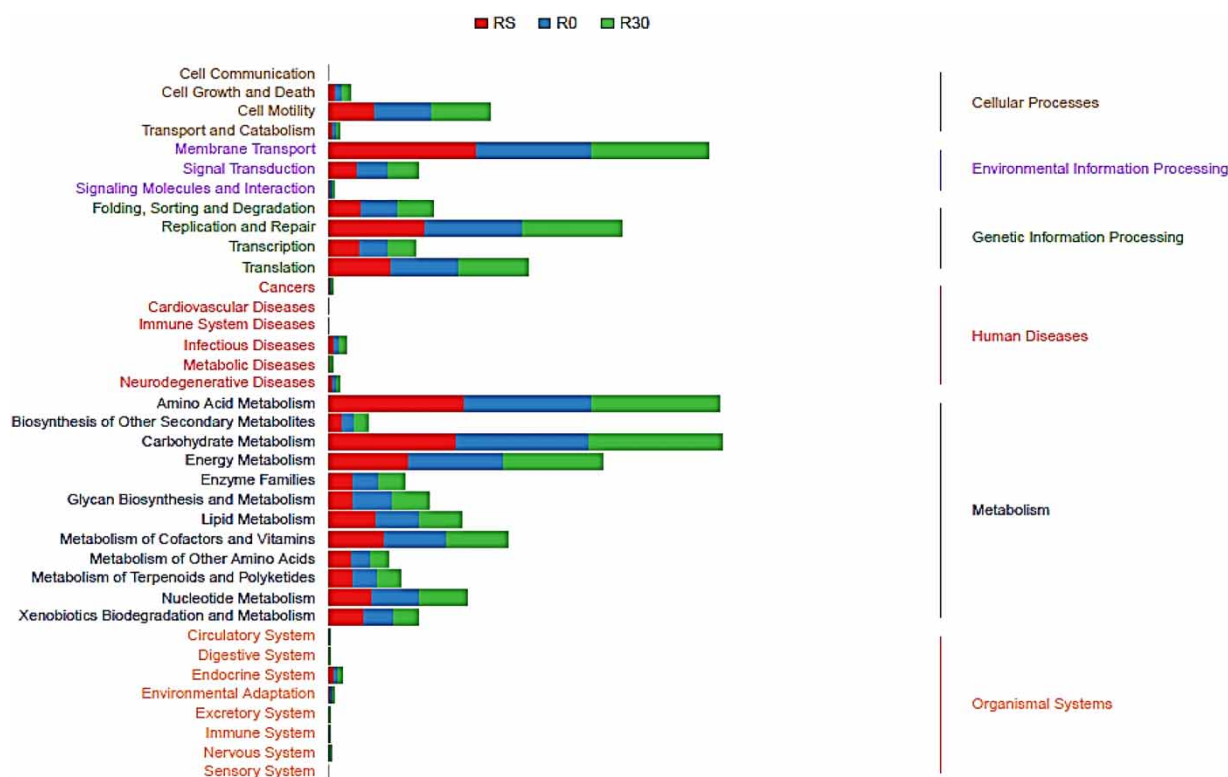


Figure 8 | Relative abundance spectra based on metabolic pathways and sub-functions.

ZVI can inhibit some microbial species and enrich functional microorganisms by affecting microbial growth and metabolism. Figure 8 shows that the microbial capacity of cell metabolism, energy metabolism, membrane transport, and cell viability of microorganisms in the presence of ZVI (R30) were higher than those in an environment devoid of ZVI (R0). These results indicated that the transfer rate and conversion rate of nitrogen related substances in R30 were faster than those in R0. Because the cells in R30 were more energetic than those in R0, nitrogen removal was improved. The ability of xenobiotics biodegradation and metabolism of R0 was significantly higher than that of R30, which may indicate that the microorganisms in R0 were degrading dead cells by heterotrophic denitrification to obtain carbon.

## CONCLUSIONS

This study examined the nitrogen removal effect and microbial influence of ZVI added to an SBR reactor treating a synthetic wastewater. The results justify the following conclusions.

ZVI significantly improves the removal of  $\text{NH}_4^+\text{-N}$  and TIN from wastewater. In the SBR reactor amended with ZVI, the highest  $\text{NH}_4^+\text{-N}$  removal efficiency was 88% and that for TIN removal was 50.12%, while the TIN removal efficiency was 29.45% higher than that in the SBR without added ZVI. ZVI also promotes the enrichment of autotrophic microorganisms such as Anammox bacteria *Candidatus Brocadia* and Feammox bacteria *Ignavibacterium*, thereby promoting the rapid construction of the autotrophic nitrogen removal system. Thus, in autotrophic SBR systems, ZVI addition promotes Anammox and Feammox reactions as nitrogen removal pathways.

## ACKNOWLEDGEMENTS

This study was funded by National Natural Science Foundation of China (No. 31802112) and the Central Public-interest Scientific Institution Basal Research Fund (No. 1610032019002).

## DATA AVAILABILITY STATEMENT

All relevant data are included in the paper or its Supplementary Information.

## REFERENCES

- APHA 2012 *Standard Methods for the Examination of Water and Wastewater*. American Public Health Association, Washington, DC, USA.
- Arcon, I., Piccolo, O., Paganelli, S. & Baldi, F. 2012 XAS analysis of a nanostructured iron polysaccharide produced anaerobically by a strain of *Klebsiella oxytoca*. *Biometals* **25** (5), 875–881.
- Batchelor, B. & Lawrence, A. W. 1978 A kinetic model for autotrophic denitrification using elemental sulfur. *Water Research* **12** (12), 1075–1084.
- Bi, Z., Qiao, S., Zhou, J., Tang, X. & Zhang, J. 2014 Fast start-up of Anammox process with appropriate ferrous iron concentration. *Bioresource Technology* **170**, 506–512.
- Biswas, S. & Bose, P. 2005 Zero-valent iron-assisted autotrophic denitrification. *Journal of Environmental Engineering* **131** (8), 1212–1220.
- Caporaso, J. G., Kuczynski, J., Stombaugh, J., Bittinger, K., Bushman, F. D., Costello, E. K., Fierer, N., Peña, A. G., Goodrich, J. K., Gordon, J. I., Huttley, G. A., Kelley, S. T., Knights, D., Koenig, J. E., Ley, R. E., Lozupone, C. A., McDonald, D., Muegge, B. D., Pirrung, M., Reeder, J., Sevinsky, J. R., Turnbaugh, P. J., Walters, W. A., Widmann, J., Yatsunenko, T., Zaneveld, J. & Knight, R. 2010 QIIME allows analysis of high-throughput community sequencing data. *Nature Methods* **7** (5), 335–336.
- Cullen, L. G., Tilston, E. L., Mitchell, G. R., Collins, C. D. & Shaw, L. J. 2011 Assessing the impact of nano- and micro-scale zerovalent iron particles on soil microbial activities: particle reactivity interferes with assay conditions and interpretation of genuine microbial effects. *Chemosphere* **82** (11), 1675–1682.
- Edgar, R. C. 2013 UPARSE: highly accurate OTU sequences from microbial amplicon reads. *Nature Methods* **10**, 996.
- Ferousi, C., Lindhoud, S., Baymann, F., Kartal, B., Jetten, M. S. & Reimann, J. 2017 Iron assimilation and utilization in anaerobic ammonium oxidizing bacteria. *Current Opinion in Chemical Biology* **37**, 129–136.
- Foglar, L. & Briški, F. 2003 Wastewater denitrification process – the influence of methanol and kinetic analysis. *Process Biochemistry* **39** (1), 95–103.
- Iino, T., Mori, K., Uchino, Y., Nakagawa, T., Harayama, S. & Suzuki, K.-i. 2010 *Ignavibacterium album* gen. nov., sp. nov., a moderately thermophilic anaerobic bacterium isolated from microbial mats at a terrestrial hot spring and proposal of *Ignavibacteria classis* nov., for a novel lineage at the periphery of green sulfur bacteria. *International Journal of Systematic and Evolutionary Microbiology* **60** (6), 1376–1382.
- Kartal, B., Kuenen, J. & Van Loosdrecht, M. 2010 Sewage treatment with anammox. *Science* **328** (5979), 702–703.
- Lee, K. C. & Rittmann, B. E. 2003 Effects of pH and precipitation on autohydrogenotrophic denitrification using the hollow-fiber membrane-biofilm reactor. *Water Research* **37** (7), 1551–1556.
- Li, J. W., Zheng, J. L., Chao, F. H., Wang, X. W., Jin, M. & Gu, C. Q. 2004 Isolation and identification of nitrite-oxidizing bacteria. *Chinese Journal of Applied & Environmental Biology* **10** (006), 786–789.
- Liu, H., Yang, F., Shi, S. & Liu, X. 2010 Effect of substrate COD/N ratio on performance and microbial community structure of a membrane aerated biofilm reactor. *Journal of Environmental Sciences* **22** (4), 540–546.
- Liu, H., Chen, Z., Guan, Y. & Xu, S. 2018 Role and application of iron in water treatment for nitrogen removal: a review. *Chemosphere* **204**, 51–62.
- Lozupone, C. & Knight, R. 2005 Unifrac: a new phylogenetic method for comparing microbial communities. *Applied and Environmental Microbiology* **71** (12), 8228–8235.
- Obaja, D., Macé, S., Costa, J., Sans, C. & Mata-Alvarez, J. 2003 Nitrification, denitrification and biological phosphorus removal in piggery wastewater using a sequencing batch reactor. *Bioresource Technology* **87** (1), 103–111.
- Qian, J., Lu, H., Cui, Y., Wei, L., Liu, R. & Chen, G.-H. 2014 Investigation on thiosulfate-involved organics and nitrogen removal by a sulfur cycle-based biological wastewater treatment process. *Water Research* **69**, 295–306.
- Ren, L. F., Ni, S. Q., Liu, C., Liang, S., Zhang, B., Kong, Q. & Guo, N. 2015 Effect of zero-valent iron on the start-up performance of anaerobic ammonium oxidation (anammox) process. *Environmental Science and Pollution Research* **22** (4), 2925–2934.
- Schinner, F., Öhlinger, R., Kandeler, E. & Margesin, R. 1996 Nitrification and denitrification. In: *Methods in Soil Biology* (F. Schinner, R. Öhlinger, E. Kandeler & R. Margesin, eds). Springer, Berlin, Heidelberg, pp. 144–161. [https://doi.org/10.1007/978-3-642-60966-4\\_10](https://doi.org/10.1007/978-3-642-60966-4_10).
- Scott, D., Hidaka, T., Campo, P., Kleiner, E., Suidan, M. T. & Venosa, A. D. 2013 Biological nitrogen and carbon removal in a gravity flow biomass concentrator reactor for municipal sewage treatment. *Chemosphere* **90** (4), 1412–1418.
- Sohn, K., Kang, S. W., Ahn, S., Woo, M. & Yang, S.-K. 2006 Fe(0) nanoparticles for nitrate reduction: stability, reactivity, and transformation. *Environmental Science & Technology* **40** (17), 5514–5519.
- Till, B. A., Weathers, L. J. & Alvarez, P. J. J. 1998 Fe(0)-supported autotrophic denitrification. *Environmental Science & Technology* **32** (5), 634–639.
- Wang, X. H., Ren, N. Q., Wang, A. J. & Ma, F. 2003 Effect of ferrous and manganese ion on nitrification. *Journal of Harbin Institute of Technology* **35** (01), 122–125.
- Wang, L., Zheng, P., Chen, T., Chen, J., Xing, Y., Ji, Q., Zhang, M. & Zhang, J. 2012 Performance of autotrophic nitrogen removal in the granular sludge bed reactor. *Bioresource Technology* **123**, 78–85.
- Wang, X., Shu, D. & Yue, H. 2016 Taxonomical and functional microbial community dynamics in an Anammox-ASBR

- system under different Fe (III) supplementation. *Applied Microbiology and Biotechnology* **100** (23), 10147–10163.
- Wang, S., Zheng, D., Wang, S., Wang, L., Lei, Y., Xu, Z. & Deng, L. 2018 Remedying acidification and deterioration of aerobic post-treatment of digested effluent by using zero-valent iron. *Bioresource Technology* **247**, 477–485.
- White, J. R., Nagarajan, N. & Pop, M. 2009 Statistical methods for detecting differentially abundant features in clinical metagenomic samples. *PLoS Computational Biology* **5** (4), e1000352.
- Windey, K., De Bo, I. & Verstraete, W. 2005 Oxygen-limited autotrophic nitrification–denitrification (OLAND) in a rotating biological contactor treating high-salinity wastewater. *Water Research* **39** (18), 4512–4520.
- Yang, W. H., Weber, K. A. & Silver, W. L. 2012 Nitrogen loss from soil through anaerobic ammonium oxidation coupled to iron reduction. *Nature Geoscience* **5** (8), 538–541.
- Yoshioka, P. M. 2008 Misidentification of the Bray-Curtis similarity index. *Marine Ecology Progress Series* **368**, 309–310.

First received 30 December 2019; accepted in revised form 29 October 2020. Available online 11 November 2020